



*Dedicated to the memory of
Dr. Emilian GEORGESCU (1946-2020)*

NEW IMIDAZOLINE DERIVATIVES, SYNTHESIS, CHARACTERIZATION AND THERMAL DEGRADATION

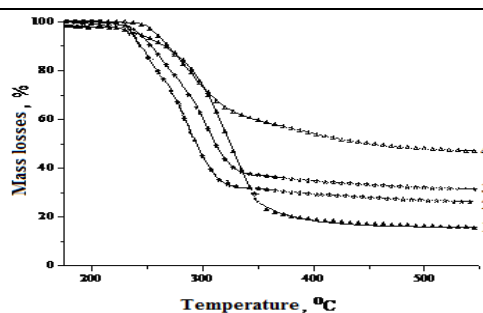
Mihaela IVANCIA^a and Anca Mihaela MOCANU^{b*}

^a“Ion Ionescu de la Brad” University of Life Sciences of Iași, Faculty of Animal Sciences, 3, Mihail Sadoveanu Alley, Iași, Roumania

^b“Gheorghe Asachi” Technical University of Iași, Faculty of Chemical Engineering and Environmental Protection, Department of Organic, Biochemical and Food Engineering, Iași, Roumania

Received June 2, 2021

The present study is intended to extend the using of substituted derivatives of the sulfonamidated phenoxyalkyl carboxylic acids to the synthesis of heterocyclic compounds. The aim is to design and synthesize pharmaceutical agents containing an imidazoline heterocyclic ring in order to develop new active pharmacological agents of high biological activities. The present study is focused on the synthesis, characterization and quantification of the environmental impact generated by the gaseous emissions of new heterocyclic derivatives with potential biological properties. The estimation of thermal stability by means of the TG-DSC-FTIR techniques is particularly important for an additional characterization of the obtained compounds.



INTRODUCTION

The imidazoline and derivatives are largely applied in the pharmaceutical,¹⁻⁸ field so that much attention has been paid lately to their synthesis. The imidazolines belong to a well-known class of biologically active compounds of growing interest, including a heterocyclic structural component responsible for their significant activities: anti-inflammatory, analgesic, anti-microbial, anti-parasitic, hypoglycemic and anticonvulsant properties.⁹⁻¹⁴ Apart from this the substituted imidazolines are also important for being largely applied in organic synthesis as intermediates, catalysts and ligands^{15,16} in various chemical reactions.^{17,18}

The imidazole ring is to be found in the basic structures of proteins, vitamins, several alkaloids and herbicides.¹⁹ Some imidazoline derivatives show interesting pharmacological properties and biological activities namely anti-hyperthyroid, anti-tumor, anti-bacterial, anti-carcinogenic and anti-inflammatory.²⁰⁻²³

Some others were applied as inhibitors of transferase, dopamine, α -glucosidase and α -amylase. New 2-imidazoline-containing monoamine oxidase MAO inhibitors are mentioned in literature,^{24,25} compounds that are important as future probes for the imidazoline binding sites of the MAOs and also for the development of new therapeutic agents.

The present paper is focused on the synthesis, characterization and investigation on the thermal

* Corresponding author: anca-mihaela.mocanu@academic.tuiasi.ro, ancamocanu2004@yahoo.com

decomposition ways of the obtained heterocyclic compounds showing potential medical and herbicidal applications. Moreover, the stages of the thermal degradation are made evident, the degradation mechanism explained and the degradation products evaluated against the environmental pollution.

By means of the TG-DSC-FTIR method every sample can be investigated making evident every stage of mass modification and purity estimation. Taking into account a single environment component, air, as the only potentially polluted component, the gaseous emissions of the tested compounds have an environmental impact whose quantification assessment was performed by applying the alternative methodology of global pollution index (I^*_{PG}).²⁶⁻²⁸ All gaseous emissions resulting from the thermal degradation released in the air must obey the environmental legislative regulations and requirements.

RESULTS AND DISCUSSION

The structures of the new derivatives

The chemical structures of the new imidazolines derivatives for which the spectral measurements and thermal stability was analyzed are presented in Figure 1.

Synthesis of the 1,2-disubstituted imidazolines involves the initial obtaining of the 2-imidazoline followed by the functionalization of the N-H group by treating with active alkylating agents or by coupling reactions with aryl halides mediated by metals. Then the sodium salts corresponding to the 2-imidazoline derivatives resulting by treating with sodium hydride in anhydrous THF were reacted with 2-chloro-methyl-imidazoline at room temperature leading to *N*-aryl-2-imidazolines.^{25,35}

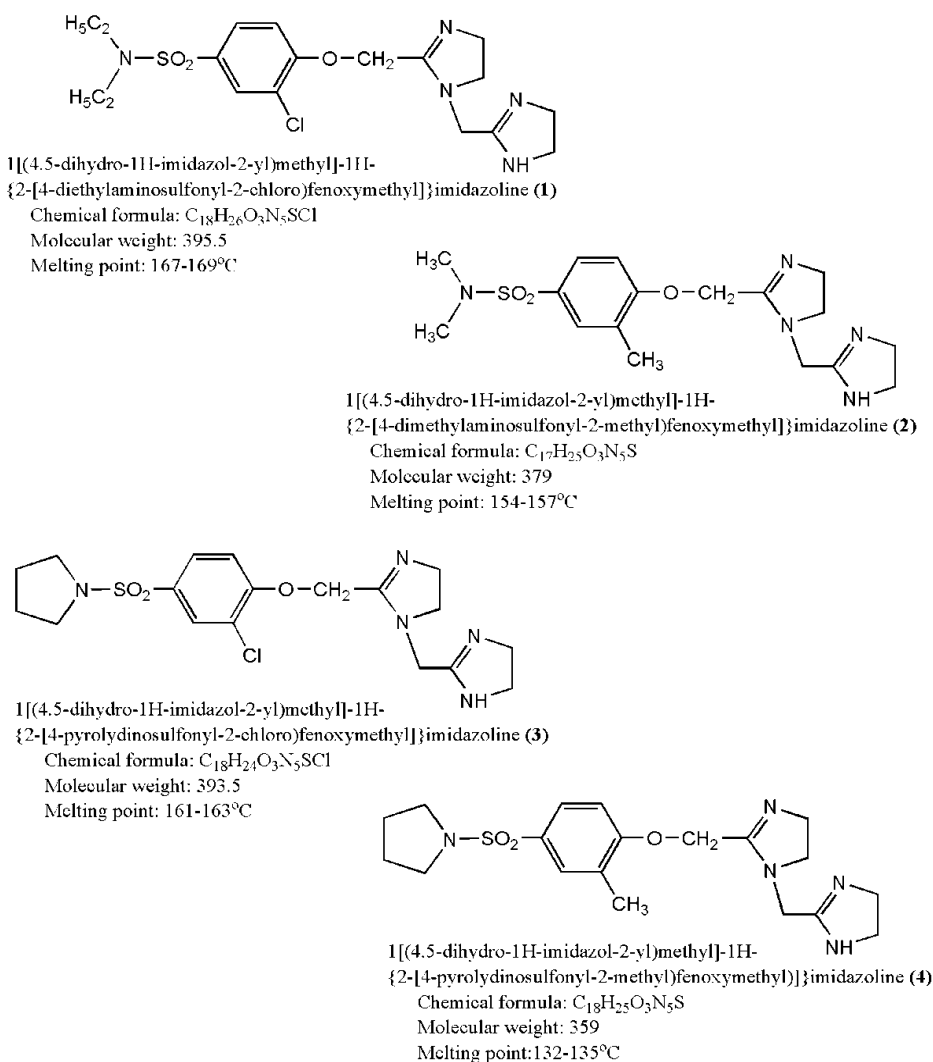


Fig. 1 – Structures of new compounds.

The newly obtained derivatives were synthesized as described in literature,²⁹⁻³⁴ by the condensation of the R₁ R₂ substituted sulfonamides of the methylic esters of the phenoxyacetic acids with ethylenediamine under acid catalysis (*p*-toluenesulfonic acid *p*-TsOH), followed by coupling the resulting derivatives with 2-chloromethylimidazoline in the presence of sodium hydride in anhydrous THF at room temperature as illustrated in the following reaction Figure 2.

By the IR, ¹H-NMR, ¹³C-NMR spectral measurements and elemental analysis were confirmed the structures of the new compounds. The spectral analyses were in good agreement with the advanced structures.

Structure elucidation by spectral measurement

IR Spectrum

In the IR spectra of the imidazoline derivatives vibration frequencies of main functional groups are to be found. For the C=N string in imidazoline ring the frequency is of 1639-1646 cm⁻¹. The absorption band for -NH group is to be found between 3244-3248 cm⁻¹.

In case of derivatives, where sulfonamidic group is entirely substituted it can be observed the band disappearance due to valency vibration of N-H. The IR spectrum of compounds were identified the vibration frequencies according to the benzene rings of 1579-1580 cm⁻¹, corresponding to

vibrations νC-C and absorptions at 3048-3050 cm⁻¹ generated by aromatic νC-H, plus intense bands of substitutes from aromatic nucleus at 1045-1055 cm⁻¹ and those of 1508-1510 cm⁻¹ of a give distorted vibration δCH₃. The Ar-O band is between 3579-3580 cm⁻¹ and in the case of S-N band is between 1675-1678 cm⁻¹. The Ar-Cl band is noticed between 1009-1012 cm⁻¹ and that of valence vibration for C-N at 1237-1239 cm⁻¹ being a very intense one.

¹H-RMN Spectrum

In the ¹H-NMR spectra the identified signals were attributed to the protons in the aromatic ring, of pyrrolidine and imidazoline cycle as well as to in the alkyl chain. The occurrence of imidazole cycle is sustained by protons signales of =N-CH₂-bonds (1.43 – 1.58 ppm); -NH- (2.1-2.3 ppm), -N-CH₂- (2.3 – 2.74 ppm), pyrrolidine cycle is sustained by protons signales of -NH- bonds (2.1 ppm) and -N-CH₂- bonds (3.32 ppm). At the same time there were identified protons in the aromatic ring (7.03-7.87 ppm) and the corresponding protons of substitutes of aromatic cycle -CH₃ (2.36-2.38 ppm) as well as to in the alkyl chain -CH₂-N- (2.56-2.58 ppm) and CH₃-CH- (0.98 ppm). The values of the chemical shifts and the intensities in the ¹H-NMR spectra are in good agreement with the proton number in the new imidazolines sintetized.

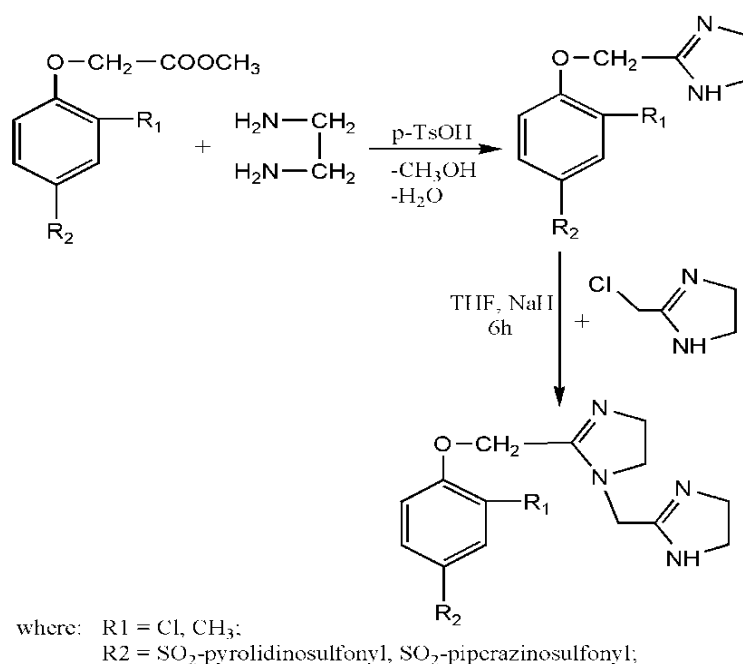


Fig. 2 – The reaction of obtaining 2-[4-(amidosulfonyl-R₁, R₂-phenoxy)methyl]-methylimidazolines

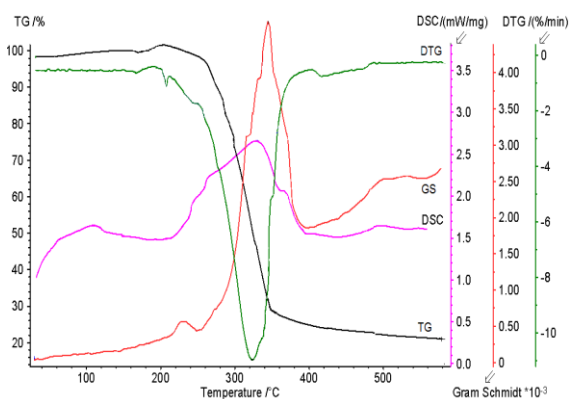


Fig. 3 – Thermograms of the sample 1.

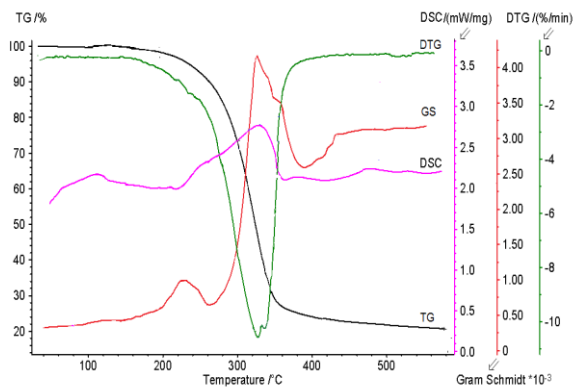


Fig. 4 – Thermograms of the sample 2.

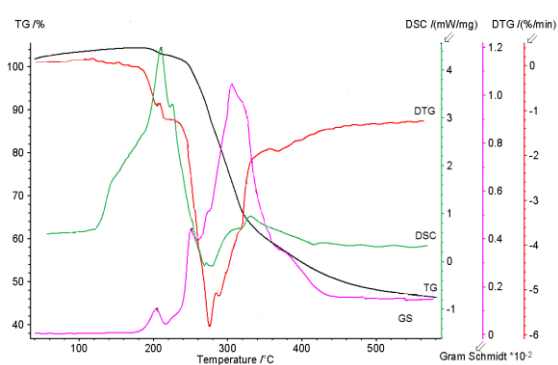


Fig. 5 – Thermograms of the sample 3.

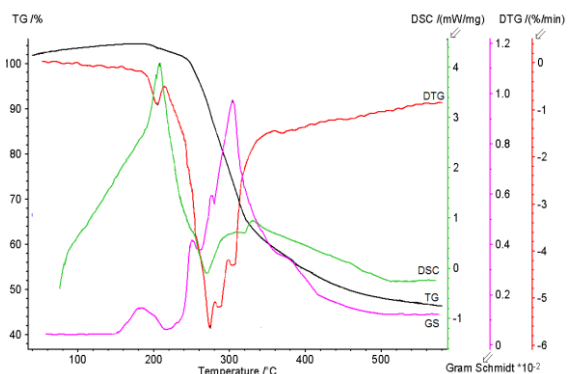


Fig. 6 – Thermograms of the sample 4.

Table 1

Characteristic amounts from TG-DTG analysis

Sample	Degradation stage	T _{onset} °C	T _{peak} °C	T _{endset} °C	W%	T ₁₀ °C	T ₅₀ °C	T _{max} (GS) °C
1	I	178	325	405	78.50	262	332	238
	residue				22.00			343
2	I	142	328	396	80.00	279	340	222
	residue				20.00			326
3	I	198	205	232	1.12	247	296	204
	II	248	276	284	14.05			254
	III residue	284	291	360	37.83 47.00			310
4	I	158	183	218	2.07	238	291	180
	II	252	276	282	9.89			242
	III	282	289	300	17.14			278
	IV residue	300	309	342	24.60 46.30			308

T_{onset} – the temperature at which the thermal decomposition begins;T_{peak} – the temperature at which the degradation rate is maximum;T_{endset} – the temperature at end of the process;T₁₀, T₅₀ – the temperature corresponding to 10 and 50 wt. % weight losses;T_{max} – temperature at which the maximum amount of gas released (from Gram-Schmidt curve);

W – weight loss.

¹³C-RMN Spectrum

In the ¹³C-RMN spectra, the imidazole cycle was confirmed by identifying the carbon signals of the

sequence -CH₂- (δ = 49.9–51.0 ppm), -C-N- (δ = 53.1 ppm), the pyrrolidine cycle was confirmed by identifying the carbon signals of the sequence – CH₂- (δ = 25.7–25.9 ppm), -C-N- (δ = 59.4–59.9

ppm), the alkyl chain shows signals at $-C-CH_3$ ($\delta = 12.9$ ppm), H_3C-N- ($\delta = 39.1$ ppm), and aromatic ring was confirmed by identifying the carbon signals of the sequence $-CH-$ ($\delta = 123.7$ and 128.7 ppm), $Ar-CH_3$ ($\delta = 14.2$ ppm), $S-Ar$ ($\delta = 133.4 - 134.1$ ppm), $Ar-O$ ($\delta = 158.7 - 160.8$ ppm).

Thermal analysis

Have been identified two temperature domains are noticed from the thermal degradation in air of the new imidazoline derivatives, namely the endothermic one, ($10-360^\circ C$) and the exothermic one ($360-600^\circ C$), domains which were grouped and also were the gaseous species resulting from the thermal degradation. The degradation process is a complex and specific one shown by the TG-DTG curve.

Within the $142-405^\circ C$ temperature range the samples are thermally degraded into some major steps within, a similarity being noticed with the samples **1** and **2**, suffering a one stage thermal degradation process while the other samples suffer a more complex degradation process.

The parameters that characterize the thermal decomposition of the samples are presented in Table 1.

From the thermal degradation it is noted that the DSC curves of the samples **1** and **2** are similar and the samples **3** and **4** are also similar.

Was noticed the same behavior of the DSC curves as that resulting from the TG-DTG analysis with the difference only that the DSC curves of all samples showed a slightly endothermic peak within the $300-360^\circ C$ range while the sample weights (from TG) did not change although a slight shift of DTG from the basic line was noticed. The

other characteristic temperatures from DSC are in agreement with those from TG-DTG.

The DSC curves show a strongly endothermic peak within the $10-215^\circ C$ range with every sample, under study where the sample mass is clearly constant corresponding to the melting interval and the temperature at the peak maximum represents the melting point. The melting points of the samples are the same within the limits of the experimental errors.

The structure of samples depend on the temperatures T_{10} (10% weight losses) which vary between $238-279^\circ C$, while T_{50} (50% weight losses) varies between $291-340^\circ C$ and the thermal stability of the compounds is differently. The weight losses varies between 24.60-80%.

This TG-FTIR method gives useful information regarding the possible impact over the environment pollution when the processing initial degradation temperature is exceeded, as for the gaseous species resulting by thermal degradation. In the TG-FTIR analysis the gaseous species were identified by means of their specific absorbance.³⁶⁻³⁸

By thermal degradation of the sample **1** under air atmosphere, is plotted for the gaseous species resulted, the absorbance versus temperature, making evident both their content in the gaseous mixture, their nature and the elimination order as well (Figure 4).

As can be seen in Figure 7, the gaseous species eliminated by thermal degradation of the new derivatives in air atmosphere within the endothermic domain ($10-360^\circ C$) are CO_2 , H_2O , NH_3 , HCl , SO_2 , intermediates (C_2H_4 , CH_2-NH-) and over the exothermic domain ($360-600^\circ C$) the gaseous species are SO_2 , CO_2 , H_2O .

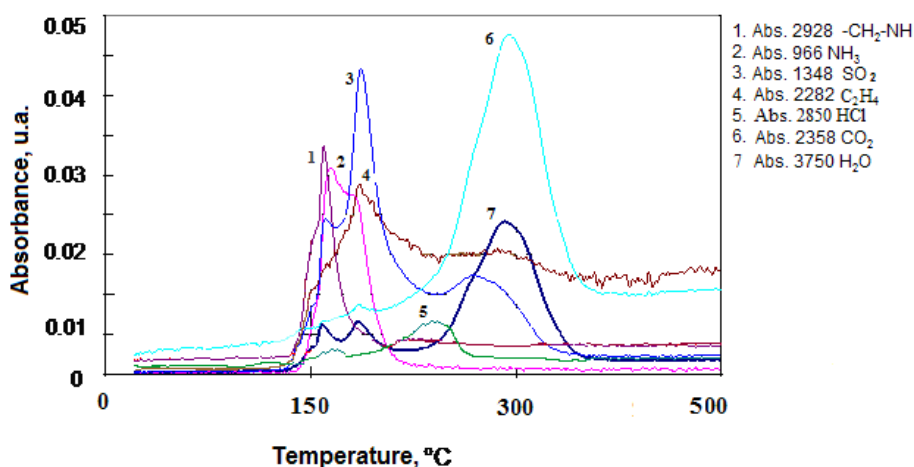


Fig. 7 – IR absorbances versus temperature for the identification of the gaseous species eliminated from the sample 1 under study.

In the endothermic domain occur the gaseous species evolved by the splitting of the covalent bonds from imidazoline derivatives, while those in the exothermal domain result by the burning of the intermediates from the endothermic process.

The most probable overall mechanism of the thermal degradation in air, based on the TG-FTIR analysis, was presented in Figure 8.

The most probable kinetic models of the degradation processes were obtained with "Multivariate Nonlinear Regression Method" (MNL). Multivariate non-linear regression program was applied for the determination of the complex mechanisms of the investigated process and kinetic parameters.

In Table 2 are presented the kinetic and statistic parameters appropriate to the tested models and

thermal degradation mechanisms. The best results were obtained by running of experimental data for conversion degree $0.1 \leq \alpha \leq 0.85$ to each selected reaction model, and considering the following conversion functions:

– reaction n-th order, model Fn:

$$f(\alpha) = (1-\alpha)^n \quad (1)$$

where: α – the conversion of thermal degradation reaction,

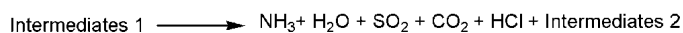
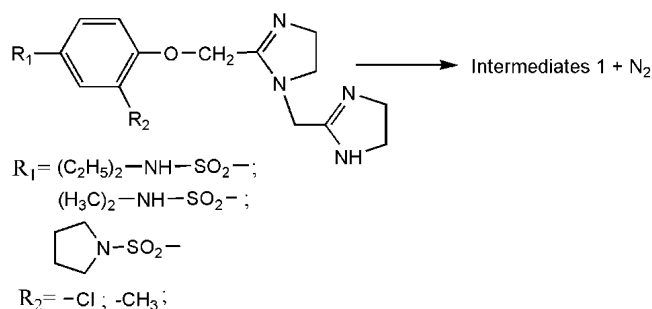
n – is the reaction order;

– Avrami –Erofeev reaction, model An:

$$f(\alpha) = n(1-\alpha)[- \ln(1-\alpha)]^{\frac{n-1}{n}} \quad (2)$$

n – is a constant parameter.

Endothermic degradation domain



Exothermal degradation domain

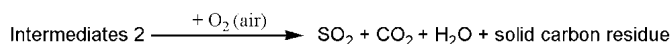


Fig. 8 – The mechanism of the thermal degradation.

Table 2

Non-isothermal kinetic and statistic parameters after MNL method and the probable mechanisms of degradation on the range 150-550°C

Parameters	Compound 1	Compound 2	Compound 3	Compound 4
	A-1→B-2→C-3→D	A-1→B-2→C-3→D	A-1→B-2→C-3→D	A-1→B-2→C-3→D
E_1/mol^{-1}	61.92	198.77	211.25	255.32
$\log A_1/\text{s}^{-1}$	3.384	16.449	18.916	23.313
dimension 1	-	0.42	0.53	0.69
n_1	0.62	-	-	-
E_2/mol^{-1}	160.53	245.82	195.36	141.69
$\log A_2/\text{s}^{-1}$	12.623	23.906	18.892	10.693
n_2	2.99	2.99	2.43	1.05
E_3/mol^{-1}	114.04	50.37	57.21	41.66
$\log A_3/\text{s}^{-1}$	7.716	1.382	0.983	0.654
n_3	0.48	1.31	1.37	1.45
FollReact. 1	0.30	0.41	0.38	0.25
FollReact. 2	0.23	0.29	0.36	0.64
$F_{\text{exp.}}$	1.00	1.00	1.00	1.00
$F_{\text{crit.}}$	1.33	1.33	1.33	1.33
correlation coefficient	0.999942	0.999956	0.999964	0.999975

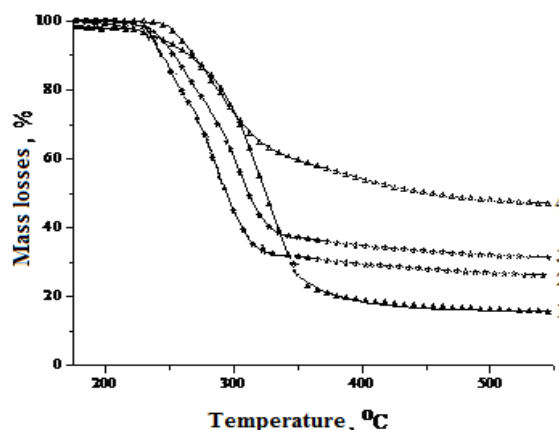
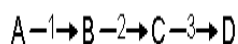


Fig. 9 – The values for the correlation coefficients (experimental value with the calculated value).

The thermal degradation follows a three steps mechanism with successive reactions of type:



(the codifications are those used in “Netzsch Thermokinetics” program: A, B, C, D are solid compounds; 1, 2, 3 denote the mechanism steps). One can notice that in both cases the thermal decomposition takes place according to some resembling kinetic models, in three phases with order n reactions.

The accuracy of kinetic parameters was checked by comparing the experimental thermograms with those simulated by computer program. There were tested more models for the thermal decomposition reactions of the samples according to “Thermokinetics 3” software (Table 2).

Figure 9 present the appropriate tested models on the temperature range 180–555°C, whose correlation coefficients are 0.999942, 0.999956, 0.999964 and 0.999975 representing a very good correlation of the experimental data with the theoretical ones. The values for the correlation coefficients being close to 1, it means the kinetic and statistic parameters have a good accuracy.

A good correlation was also noticed between the structure, thermal stability appreciated from the initial degradation temperatures from TG and DTG and the degradation mechanism. The thermal degradation mechanisms of the samples are complex and specific developing by successive simultaneous reactions depending on the structure and nature of the substitutes in the molecule.

The quantification of the evaluation of the environment impact (EIM) generated by the thermal degradation of the imidazolines under study was performed by applying the alternative methodology of the global, pollution index (I_{PG}^*).

The global status of the atmosphere component can be evaluated by means of the global pollution index (I_{PG}^*).³⁹

$$I_{PG}^* = \frac{100}{\overline{ES}_{air}^2} \quad (3)$$

where: \overline{ES}_{air}^2 – the arithmetic average of the square values of the evaluation score for every quality index under consideration.

Are given in Table 3 based on the correlation between the value of the global pollution index I_{PG}^* and the real pollution state of the atmospheric air, the values of the \overline{ES}_{air}^2 , global pollution index I_{PG}^* and the estimation of the real pollution state.

All gaseous species eliminated by the thermal degradation can be regarded as air quality pollutants, some of them having a toxic to lethal effect on human health in case of long-term exposure.

The concentration values of the compounds resulting by thermal degradation which are regarded as air quality indicators are measured, the evaluation consisting mainly in the calculation of an index expressing the air quality at the emission source, EQ_i :

$$EQ_i = C_{i,measured} / M.A.C_i \quad (4)$$

where:

i – identification number of every gas component resulting by thermal degradation;

$C_{i,measured}$ – experimental concentration of the resulting gas component;

M.A.C_i – the maximum admitted concentration of the gas component according to the environmental legislative rule.^{40,41}

Table 3

The estimation of the real situation of the air pollution

No.	New tested products / abbreviation	\overline{ES}_{air}^2	I^*_{PG} value	Real situation of the air pollution
1	Compound 1	67.2400	1.4872	1 < I^*_{PG} < 2 Air environment modified by thermal degradation activities within admissible limits
2	Compound 2	64.0000	1.5625	
3	Compound 3	67.2400	1.4872	
4	Compound 4	60.0625	1.6649	

Table 4

The compounds of thermal degradation evaluated for estimating the global impact of the discharges in air

Thermal degradation compounds	M.A.C. ^a (mg.m ⁻³)x10 ⁻³	Air quality index (EQ _i) (for the compounds)				Evaluation Score (ES _i) (for the compounds)			
		1	2	3	4	1	2	3	4
NH ₃	30	0.0730	0.0761	0.0733	0.0804	9	9	9	9
SO ₂	500	0.0164	0.0172	0.0165	0.0181	9	9	9	9
CO ₂	100.000.000 kg/an ^b	-	-	-	-	-	-	-	-
HCl	30	0.1567	-	0.1575	-	9	-	9	-
CH ₂ NH-	1	3.7362	3.8989	3.7549	4.1156	5	5	5	4
C ₂ H ₄	150	0.0240	0.0250	0.0241	0.0264	9	9	9	9
		EQ _{1,air} = 0.6677	EQ _{2,air} = 0.6695	EQ _{3,air} = 0.6710	EQ _{3,air} = 0.7067	ES _{1,air} = 8.2	ES _{2,air} = 8	ES _{3,air} = 8.2	ES _{3,air} = 7.75

Are given in Table 4, the analyzed gaseous components, the value of the quality index (EQ_i) and the evaluation score (ES_i).

The gaseous species evolved by thermal degradation of the imidazolines have been estimated for the 10-400°C temperature range and compared subsequently with the maximum admissible concentrations (M.A.C) given by the actual environment rules. These amounts were also individually evaluated, for each compound, as well as de impact on the environment exerted by de synergetic action of all polluting gaseous species released.

By evaluation score in air ES_i, is the characterized every variation range EQ_i.⁴² Representing an irreversible major degradation state of the atmosphere and the natural unaffected state, respectively, the minimum and maximum values of the evaluation score, ES_i, are of 1 and 10, respectively.^{26,27}

EXPERIMENTAL

Materials

Starting materials and solvents were obtained commercially and used as received. All reagents and solvents had purity grade and were obtained from commercial suppliers. The esters has be sintetized and has of high purity. Melting points were determined in open capillaries in electrical melting point

apparatus and are uncorrected. Elemental analyses were carried out using a Perkin Elmer CHNS/O Analyzer Series II 2400 apparatus, and the results were within ± 0.4% of theoretical values. ¹H-NMR and ¹³C-NMR spectra of the compounds were recorded in DMSO-d₆ using Bruker Avance 300 MHZ and and 75 MHZ instrument. Chemical shifts are reported in parts per million (δ units) downfield/upfield from residual DMSO (δ 2.50 and 39.5); coupling constants (J) are reported in hertz (Hz).

The chemical shifts were expressed in ppm using tetramethylsilane (TMS) as internal standard. Spin multiplets are given as: s (singlet), d (doublet). FT-IR spectra were performed on a Biorad FT-IR- FTS 570°C spectrometer.

Thermogravimetric measurements (TGA) were performed on a Mettler Toledo TGA-SDTA851e derivatograph (thermogravimetric analyzer) under a flow of air (20 mL/min), in the temperature range 10–600°C, and a heating rate of 10 K min⁻¹ with 10 mg of sample mass. The TG/DTG instrument was calibrated with standards weights according to the manufacturer proceedings. Thermal degradation of some imidazoline derivatives and evolved gas analyses were performed using a TG/FTIR. The system is equipped with an apparatus of simultaneous thermogravimetric spectrophotometer FTIR model Vertex-70 (Bruker-Germany). Samples with weight ranging from 7-10 mg were heated from 10 to 600°C, at a heating rate of 10°C/min.

Synthesis

General procedure for the preparation of 2-imidazolines-N-arilates

The R₁,R₂-substituted methylic esters of the phenoxyacetic acids were solved in anhydrous methanol and then the *p*-TsOH and ethylenediamine in anhydrous methanol added. The resulting reaction mixture was refluxed for 4 hours, the

methanol removed under vacuum, the remaining residue treated with water and then let to stay till crystallization. The 4-(amidosulfonyl-R₁,R₂-phenoxyethyl)-2-imidazoline derivatives thus obtained were finally purified by repeated recrystallizations from water. To the 4-(amidosulfonyl-R₁,R₂-phenoxyethyl)-2-imidazoline solved in anhydrous THF the sodium hydride was added at room temperature and the 2-(chloromethyl)-4,5-dihydro-1H-imidazole added 15 minutes later stirring then the reaction mixture for 6 hours at room temperature. The resulting *N*-alkylated products were separated by water addition followed by extraction with dichloromethane.²⁹⁻³⁴

Synthesis of the 1[(4,5-dihydro-1H-imidazol-2-yl)methyl]-1H-2-[4-diethylaminosulfonyl-2-chloro]phenoxyethyl]imidazoline (1)

A white solid, mp = 167–169°C; Anal. Calcd (C₁₈H₂₄O₃N₆SCl): C, 49.14; H, 5.46; N, 19.11. Found: C, 49.06; H, 5.52; N, 19.08; FT-IR (KBr, cm⁻¹): 1012 (Ar-Cl), 1045 (C-H), 1140 (-SO₂-N-), 1229 (C-S), 1239 (-C-N-), 1248 (-C-O-), 1386 (δ C-H), 1579 (-C-C-), 1600 (C=C), 1646 (-C=N-), 3048 (δ C-H), 3245 (-NH-), 3579 (Ar-O-) cm⁻¹; H-NMR δ/ppm (400 MHz, DMSO): 0.98 (d, 3H, -CH₃), 1.43 (s, 2H, =N-CH₂- of imidazole), 1.58 (s, 2H, =N-CH₂- of imidazole), 2.3 (s, 1H, -NH- of imidazole), 2.56 (s, 2H, -N-CH₂- of imidazole), 2.58 (s, 2H, -N-CH₂-), 2.74 (s, 2H, -N-CH₂- of imidazole), 3.24 (d, 2H, -CH₂-), 3.94 (s, 2H, -O-CH₂-), 7.03 (s, H, Ar-H), 7.67 (s, H, Ar-H), 7.87 (s, H, Ar-H); ¹³C-NMR δ/ppm (DMSO-d₆): δ= 12.9 (H₃C-C-), δ= 38.4 (-CH₂-N-), δ= 49.9 and δ= 51.0 (-CH₂- of imidazole), δ= 53.1 (-N-C- of imidazole), δ=75.9 (-O-CH₂-), δ= 123.7 and 128.7 (CH aromate ring), δ=134.1 (-S-Ar), δ= 159.8 (Ar-O), δ= 162.8 (-CH₂- of imidazole).

Synthesis of the 1[(4,5-dihydro-1H-imidazol-2-yl)methyl]-1H-2-[4-dimethylaminosulfonyl-2-methyl]phenoxyethyl]imidazoline (2)

A white solid, mp = 154–157°C; Anal. Calcd (C₁₉H₂₇O₃N₆S): C, 54.41; H, 6.44; N, 20.04. Found: C, 54.38; H, 6.48; N, 19.98; FT-IR (KBr, cm⁻¹): 1048 (C-H), 1139 (-SO₂-N-), 1230 (C-S), 1238 (-C-N-), 1247(-C-O-), 1385 (δ C-H), 1508 (Ar-CH₃), 1580 (-C-C-), 1601 (C=C), 1644 (-C=N-), 3050 (ν C-H), 3246 (-NH-), 3580 (Ar-O-) cm⁻¹; ¹H-NMR δ/ppm (400 MHz, DMSO): 1.43 (s, 2H, =N-CH₂- of imidazole), 1.58 (s, 2H, =N-CH₂- of imidazole), 2.35 (s, 1H, -NH- of imidazole), 2.38 (s, 3H, -CH₃), 2.43 (d, 3H, -CH₃), 2.56 (s, 2H, -N-CH₂- of imidazole), 2.57 (s, 2H, -N-CH₂-), 2.73 (s, 2H, -N-CH₂- of imidazole), 3.95 (s, 2H, -O-CH₂-), 7.03 (s, H, Ar-H), 7.67 (s, H, Ar-H), 7.87 (s, H, Ar-H); ¹³C-NMR δ/ppm (DMSO-d₆): δ= 14.2 (H₃C-Ar), δ= 39.1 (H₃C-N-), δ= 49.9 and δ= 51.0 (-CH₂- of imidazole), δ= 53.1 (-N- of imidazole C-), δ= 75.8 (-O-CH₂-), δ= 123.7 and 128.7 (CH aromate ring), δ= 133.4 (-S-Ar), δ= 160.8 (Ar-O), δ= 162.8 (-CH₂- of imidazole).

Synthesis of the 1[(4,5-dihydro-1H-imidazol-2-yl)methyl]-1H-2-[4-pyrrolydinosulfonyl-2-chloro]phenoxyethyl]imidazoline (3)

A white solid, mp = 161–163°C; Anal. Calcd (C₁₈H₂₄O₃N₅SCl): C, 50.76; H, 5.64; N, 16.45. Found: C, 49.06; H, 5.52; N, 19.08; FT-IR (KBr, cm⁻¹): 1009 (Ar-Cl), 1052 (C-H), 1229 (C-S), 1239 (-C-N-), 1247 (-C-O-), 1385 (δ C-H), 1579 (-C-C-), 1600 (C=C), 1639 (-C=N-), 1675 (-SO₂-N-ring), 3048 (ν C-H), 3244 (-NH-), 3579 (Ar-O-) cm⁻¹; H-NMR δ/ppm (400 MHz, DMSO): 1.43 (s, 2H, =N-CH₂- of

imidazole), 1.57 (s, 2H, =N-CH₂- of imidazole), 2.1 (s, 1H, -NH- of pyrrolydine), 2.3 (s, 1H, -NH- of imidazole), 2.56 (s, 2H, -N-CH₂- of imidazole), 2.58 (s, 2H, -N-CH₂-), 2.65 (d, 2H, Ar-H), 2.73 (s, 2H, -N-CH₂- of imidazole), 3.32 (d, 2H, -CH₂-N of pyrrolydine), 3.95 (s, 2H, -O-CH₂-), 7.03 (s, H, Ar-H), 7.67 (s, H, Ar-H), 7.87 (s, H, Ar-H); ¹³C-NMR δ/ppm (DMSO-d₆): δ= 25.7 (-CH₂- of pyrrolydine), δ= 49.9 and δ= 51.0 (-CH₂- of imidazole), δ= 53.1 (-N-C- of imidazole), δ= 59.0 (-CH₂-N- of pyrrolydine), δ= 74.7 (-O-CH₂-), δ= 123.7 and 128.7 (CH aromate ring), δ= 134.1 (-S-Ar), δ= 158.7 (Ar-O-), δ= 162.8 (-CH₂- of imidazole).

Synthesis of the 1[(4,5-dihydro-1H-imidazol-2-yl)methyl]-1H-2-[4-pyrrolydinosulfonyl-phenoxyethyl]imidazoline (4)

A white solid, mp = 132–135°C; Anal. Calcd (C₁₈H₂₅O₃N₅S): C, 55.24; H, 6.39; N, 17.90. Found: C, 49.06; H, 5.52; N, 19.08; FT-IR (KBr, cm⁻¹): 1055 (C-H), 1231 (C-S), 1237 (-C-N-), 1246 (-C-O-), 1384 (δ C-H), 1510 (Ar-CH₃), 1579 (-C-C-), 1602 (C=C), 1643 (-C=N-), 1678 (-SO₂-N-ring), 3049 (ν C-H), 3248 (-NH-), 3580 (Ar-O-); H-NMR δ/ppm (400 MHz, DMSO): 1.43 (s, 2H, =N-CH₂- of imidazole), 1.57 (s, 2H, =N-CH₂- of imidazole), 2.1 (s, 1H, -NH- of pyrrolydine), 2.1 (s, 1H, -NH- of imidazole), 2.36 (s, 3H, -CH₃), 2.56 (s, 2H, -N-CH₂- of imidazole), 2.58 (s, 2H, -N-CH₂-), 2.65 (d, 2H, Ar-H), 2.73 (s, 2H, -N-CH₂- of imidazole), 3.32 (d, 2H, -CH₂-N of pyrrolydine), 3.96 (s, 2H, -O-CH₂-), 7.03 (s, H, Ar-H), 7.67 (s, H, Ar-H), 7.87 (s, H, Ar-H); ¹³C-NMR δ/ppm (DMSO-d₆): δ= 14.2 (H₃C-Ar), δ= 25.9 (-CH₂- of pyrrolydine), δ= 49.9 and δ= 51.0 (-CH₂- of imidazole), δ= 53.1 (-N-C- of imidazole), δ= 58.5 (-CH₂-N- of pyrrolydine), δ= 74.5 (-O-CH₂-), δ= 123.7 and 128.7 (-CH- aromate ring), δ= 134.1 (-S-Ar), δ= 158.9 (Ar-O-), δ= 162.8 (-CH₂- of imidazole).

CONCLUSIONS

The present work reports the synthesis, spectral characterization, thermal degradation and the quantification of environmental impact assessment of newly synthesized imidazoline derivatives.

The reactions describing herein the synthesis methods of imidazoline derivatives open new opportunities for their applications in the fields of medicine, agriculture, theoretical and synthetic organic chemistry.

Thus the compounds containing imidazoline ring can be regarded as compounds showing pesticide properties, significant anti-inflammatory and analgesic actions which could be useful in finding new drugs as well as in developing potential applications in anti-inflammatory therapy.

The studies on the thermal degradation of the newly obtained compounds are useful for estimating their use at high temperatures as well as the product life time.

The TG-DTG-DSC curves obtained with the imidazolines derivatives under study are indicative of complex and specific degradation mechanisms and consequently of the structure influence. The

gaseous species evolved by degradation and those resulting from thermal analysis are in good agreement.

The thermal stability depends on the chemical structure of the new imidazoline derivatives making thus possible to ascertain the temperature range proper for using and storing.

The value of the global pollution index, I^*_{PG} , represents a crucial indicator making evident the modification of the atmospheric environment within the allowed limits by the gases resulting by the thermal degradation.

REFERENCES

1. M. Y. Wang, Y. Y. Jin, H. Y. Wei, L. S. Zhang, S. X. Sun, X. B. Chen, W. L. Dong, W. R. Xu, X. C. Cheng and R. L. Wang, *Eur. J. Med. Chem.*, **2015**, *103*, 91-104.
2. M. Fondo, J. Doejo, A. M. García-Deibe, J. Sanmartín, C. González-Bello and R. Vicente, *Polyhedron*, **2015**, *100*, 49-58.
3. G. Wang, Y. Wang, L. Wang, L. Han, X. Hou, H. Fu and H. Fang, *Bioorg. Med. Chem.*, **2015**, *23*, 7359-7365.
4. J. M. Coustard, Y. Soro, S. Siaka, F. Bamba and A. Cousson, *Tetrahedron*, **2006**, *62*, 3320-3328.
5. Y. Brouillette, V. Lisowski, J. Guillon, S. Massipb and J. Martinez, *Tetrahedron*, **2007**, *63*, 7538-7544.
6. R. De La Rosa, V. Martinez-Barraza, C. Burgos and J. Alvarez-Builla, *Tetrahedron Lett.*, **2000**, *41*, 5837-5840.
7. M. Naka, T. Nanbu, K. Kobayashi, Y. Kamanaka, M. Komeno, R. Yanasa, T. Fukutomi, S. Fujimura, N. G. Seo, N. Fujiwara, S. Ohuchida, K. Suzuki, K. Kondo and N. Taniguchi, *Biochem. Biophys. Res. Commun.*, **2000**, *270*, 663-667.
8. J. A. Tucker, T. L. Clyton, C. G. Chidester, M. W. Schulz, L. E. Harrington, S. J. Conrad, Y. Yagi, N. L. Oien, D. Yurek and M. S. Kuo, *Bioorg. Med. Chem.*, **2000**, *8*, 601-615.
9. H. Xie, J. C. Liu, L. Wu and M. W. Ding, *Tetrahedron*, **2012**, *68*, 7984-7990.
10. R. Sarges and P. Oates, "Progrese in Drug Research", Vol. 40, Birkhäuser Verlag, Basel, 1993, p. 99-161.
11. L. Somsak, L. Kovacs, M. Toth, E. Osz, L. Szilagy, Z. Gyorgydeak, Z. Dinya, T. Docsa, B. Toth and P. Gergely, *J. Med. Chem.*, **2001**, *44*, 2843-2848.
12. C. H. Kwon, M. T. Iqbal and J. N. D. Worpel, *J. Med. Chem.*, **1991**, *34*, 1845-1849.
13. N. Opacic, M. Barbaric, B. Zorc, M. Cetina, A. Nagy, D. Frkovic, M. Kralj, K. Pavelic, J. Balzarini, G. Andrei, R. Snoeck, E. De Clercq, S. Raic-Malic and M. Mintas, *J. Med. Chem.*, **2005**, *48*, 475-482.
14. G. Roy, D. Das and G. Mugesh, *Inorg. Chim. Acta*, **2007**, *360*, 303-316.
15. P. Bousquet and J. Feldman, *Drugs*, **1999**, *58*, 799-812.
16. T. Isobe, K. Fukuda, Y. Araki and T. Ishikawa, *Chem. Commun.*, **2001**, 243-244.
17. D. Ciubotariu and M. Nechifor, *Rev. Med. Chir. Soc. Nat.*, **2012**, *116*, 1118-1122.
18. M. Ueno, K. Imaizumi, T. Sugita, I. Takata and M. Takeshita, *Int. J. Immunopharmacol.*, **1995**, *17*, 597-603.
19. F. Rondou, S. Le Bihan, G. X. Wang, A. Lamouri, E. Touboul, G. Dive, T. Bellahsene, B. Pfeiffer, P. Renard, B. Guardiola-Lemaitre, D. Manechez, L. Penicaud, A. Ktorza and J. J. Godfroid, *J. Med. Chem.*, **1997**, *40*, 3793-3803.
20. C. Congiu, M. T. Cocco and V. Onnis, *Bioorg. Med. Chem. Lett.*, **2008**, *18*, 980-993.
21. A. Saeed and M. Batool, *Med. Chem. Res.*, **2007**, *16*, 143-154.
22. T. R. Sharpe, S. C. Cherkofsky, W. E. Hewes, D. H. Smith, W. A. Gregory, S. B. Haber, M. R. Leadbetter and J. G. Whitney, *J. Med. Chem.*, **1985**, *28*, 1188-1194.
23. M. Wozzakowska, M. Sztanke and K. Sztanke, *J. Anal. Applied. Pyrolysis*, **2019**, *143*, 104686-104691.
24. A. Shetnev, A. Osipyany, S. Baykov, A. Sapagin, Z. Chirkova, M. Korsakov, A. Petzer, I. Engelbrecht and J. P. Petzer, *Bioorg. Med. Chem. Lett.*, **2018**, *29*, 40-46.
25. C. Binda, P. Newton-Vinson, F. Hubalek, D. E. Edmondson and A. Mattevi, *Nat. Struct. Biol.*, **2002**, *9*, 22-26.
26. M. Macoveanu, "Metode și Tehnici de Evaluare a Impactului Ecologic", Ediția a II-a, Editura Ecozone, Iași, Roumania, 2005.
27. C. Popa, C. Cojocaru and M. Macoveanu, *Environ. Eng. Manag. J.*, **2005**, *4*, 437-447.
28. C. Zaharia and M. Surpateanu, *Environ. Eng. Manag. J.*, **2006**, *5*, 1141-1152.
29. C. Soldea, C. Oniscu and V. Sunel, *Rev. Med. Chir. Soc. Med. Nat.*, **1992**, *96*, 265-268.
30. V. P. Radha, S. J. Kirubavathy and S. Chitra, *J. Mol. Struct.*, **2018**, *1165*, 246-258.
31. G. Lazorenko, A. Kasprzhitskii and V. Yavna, *Chem. Phys. Lett.*, **2018**, *692*, 264-270.
32. G. Caprioli, V. Mammoli, M. Ricciutelli, G. Sagratini, M. Ubaldi, E. Domi, L. Mennuni, C. Sabatini, C. Galimberti, F. Ferrari, C. Milia, E. Comi, M. Lanza, M. Giannella, M. Pigni and F. Del Bello, *Eur. J. Pharmacol.*, **2015**, *769*, 219-224.
33. R. G. Campbell, S. Nair, R. Sacks and R. G. Douglas, *Med. Hypot.*, **2014**, *82*, 706-708.
34. R. Li, H. Jiang, W. Y. Liu, P. M. Gu and X.Q. Li, *Chin. Chem. Lett.*, **2014**, *25*, 583-585.
35. J. Saczewski, A. Hudson, M. Scheinin, A. Rybczynska, D. Mae, F. Saczewski, S. Laird, J. M., Laurila, K. Boblewski, A. Lehmann, J. Gu and H. Watts, *Bioorg. Med. Chem.*, **2012**, *20*, 108.
36. A. M. Mocanu and C. Luca, *Rev. Chim. (Bucharest)*, **2014**, *65*, 185-189.
37. A. M. Mocanu, L. Odochian, C. Moldoveanu and G. Carja, *Therm. Acta*, **2010**, *509*, 33-39.
38. A. M. Mocanu, L. Odochian, N. Apostolescu and C. Moldoveanu, *J. Therm. Anal. Calorim.*, **2011**, *103*, 283-291.
39. C. Zaharia and I. Murarasu, *Environ. Eng. Manag. J.*, **2009**, *8*, 107-112.
40. C. Zaharia, "Legislation for environment protection", 'Al. I. Cuza' University Press, Iași, Roumania, 2003.
41. C. Zaharia, "Legislation for environment protection", Politehnic Press, Iași, Roumania, 2008.
42. A. Grec, F. Dumescu and C. Maior, *Environ. Eng. Manag. J.*, **2009**, *8*, 1533-1540.